HUMAN GENE THERAPY 14:871–881 (June 10, 2003)

Pathways of Removal of Free DNA Vector Ends in Normal and DNA-PKcs–Deficient SCID Mouse Hepatocytes Transduced with rAAV Vectors

HIROYUKI NAKAI, THERESA A. STORM, SALLY FUESS, and MARK A. KAY

ABSTRACT

Elucidation of the mechanisms of transformation of single-stranded (ss) recombinant adeno-associated virus (rAAV) vector genomes into a variety of stable double-stranded (ds) forms is key to a complete understanding of rAAV vector transduction *in vivo*. Ds monomer genome formation and cellular ds DNA break (DSB) repair pathways that remove free vector ends toxic to cells, presumably play a central role in this process. By delivering rAAV and naked ds linear DNA vectors into livers of DNA-dependent protein kinase catalytic subunit (DNA-PKcs)–deficient severe combined immunodeficiency (SCID) and wild-type mice, we demonstrate the presence of three major pathways for free ds vector end removal: (1) DNA-PKcs–dependent self-circularization, (2) DNA-PKcs–independent self-circularization, and (3) DNA-PKcs-independent concatemerization. By using the DNA-PKcs–independent pathways, mouse hepatocytes efficiently removed free ds rAAV vector ends even in the absence of DNA-PKcs. Our studies suggest a hierarchical organization of these processes; self-circularization is the preferred pathway over concatemerization, although the former has a limited capacity to remove free vector ends. These studies shed new light on the molecular mechanisms of rAAV vector transduction *in vivo*.

OVERVIEW SUMMARY

Recombinant AAV (rAAV) vector genome processing, an important step toward stable transduction, relies totally on host cellular machinery such as DNA repair systems. We presume that double-stranded (ds) rAAV vector genomes in stably transduced cells (circular monomers, concatemers, and integrated forms) are byproducts generated by host defense mechanisms designed to remove free ends of broken ds DNA. In the present study, by comparing rAAV and naked ds linear DNA transduction in the livers of DNA-dependent protein kinase catalytic subunit (DNA-PKcs)–deficient severe combined immunodeficiency (SCID) and wild-type mice, we demonstrate that DNA-PKcs is a key protein but not necessarily essential for free vector end removal in mouse hepatocytes *in vivo*. In addition, we show the presence of a DNA-PKcs–independent self-circularization pathway(s), which has a limited capacity, but is preferentially utilized over the concatemerization pathway with a much larger capacity for processing free ds DNA ends.

INTRODUCTION

RECOMBINANT ADENO-ASSOCIATED VIRUS (rAAV) vectors are of great interest for human gene therapy because they are based on a nonpathogenic virus that can be delivered safely and directly into human subjects, resulting in persistent expression of therapeutic products (Kay *et al.*, 2000; Stedman *et al.*, 2000; Arruda *et al.*, 2001; Wagner *et al.*, 2002). The vector is permissive in two major target organs, skeletal muscle and liver, and in both tissues, single-stranded (ss) rAAV vector genomes transform into a variety of double-stranded (ds) vector forms (i.e., ds linear monomers, ds circular monomers, ds linear and circular concatemers), and integrated forms (Xiao *et al.*, 1996; Duan *et al.*, 1998; Miao *et al.*, 1998; Nakai *et al.*, 1999, 2000, 2002; Sanlioglu *et al.*, 1999; Vincent-Lacaze *et al.*, 1999; Yang *et al.*, 1999; Malik *et al.*, 2000). Among them, ds linear rAAV monomers are presumed to be a key intermediate toward the abovementioned various vector forms (Nakai *et al.*, 2003a,b), and circular monomer rAAV genomes appear to be most responsible for persistent transgene expression (Duan *et al.*, 1998;

Departments of Pediatrics and Genetics, Stanford University School of Medicine, Stanford, CA 94305.

Nakai *et al.*, 2001, 2002). However, the factors that drive vector genome processing remain to be elucidated.

Recently several cellular proteins have been shown to be associated with rAAV viral genomes. Qing *et al.* demonstrated that FKBP52 protein specifically binds to AAV inverted terminal repeat D region, which inhibits viral genome second-strand synthesis when phosphorylated (Qing *et al.*, 1997, 2001). The proteins involved in ds DNA break (DSB) repair systems have been suggested to bind to rAAV vector genomes, because vector transduction is significantly increased by ionizing irradiation or genotoxic drugs (Alexander *et al.*, 1994, 1996), or in the absence of the ataxia telangiectasia gene product that functions as a guardian for cell cycling (Sanlioglu *et al.*, 2000). Recently Song *et al.* (2001) reported that in the absence of DNA-dependent protein kinase catalytic subunit (DNA-PKcs), removal of free vector ends (ds DNA ends) is impaired, resulting in persistence of ds linear rAAV vector genomes in DNA-PKcs–deficient severe combined immune deficiency (SCID) mouse skeletal muscle. On the other hand, Zentilin and colleagues (2001) reported that other ds DNA break binding proteins, Ku86 and Rad52, can associate with rAAV genomes in transduced cells, and found that rAAV transduction is increased and decreased in Ku86- and Rad52-deficient cells, respectively. Although the roles of such DSB repair proteins in rAAV transduction are not well understood, these previous studies have provided further insights into the involvement of DSB repair pathways in rAAV transduction.

DNA-PKcs is a pivotal component of the nonhomologous end-joining (NHEJ) DSB repair pathway, and lack of normal DNA-PKcs catalytic activity affects V(D)J recombination during lymphocyte maturation (Blunt *et al.*, 1996; Danska *et al.*, 1996), which markedly reduces numbers of both mature B and T lymphocytes, resulting in the SCID phenotype (Bosma *et al.*, 1983). CB17 SCID, used in the previous (Song *et al.*, 2001) and present study, was originally discovered in a colony of CB17 mice as a spontaneous germline mutation (Bosma *et al.*, 1983). The mutation resides in the DNA-PKcs, deleting 83 amino acids from the C terminus of this protein, and inactivates the catalytic activity. Recently, several reports have been published claiming that DNA-PKcs plays an important role in retrovirus integration, and lack of DNA-PKcs activity reduces integration efficiency and induces apoptosis (Daniel *et al.*, 1999, 2001). These studies shed new light on the involvement of cellular repair systems in viral life cycles (Coffin and Rosenberg, 1999).

Because rAAV vectors do not carry or express virally encoded recombinase, the transformation of ds linear rAAV vector genomes into a variety of stable forms (circular monomers, concatemers and integrated forms) totally depends on host cellular recombination machinery. The presence of DSB in host chromosomal DNA is life-threatening to cells, and serves as a proapoptotic signal if not repaired (Huang *et al.*, 1996; Smith and Jackson, 1999). Because free ds DNA ends generated by viral infection, such as the termini of retroviral linear cDNA and AAV, serve as a DSB signal (Daniel *et al.*, 1999; Li *et al.*, 2001; Raj *et al.*, 2001) and a single unrepaired DSB can be lethal to cells (Bennett *et al.*, 1993), vector-transduced cells manage to remove free vector ends not only by degradation but also by ligating free DNA ends into a contiguous DNA strand. Based on this, we presume that various ds rAAV genomes found in stably transduced hepatocytes could all be byproducts generated by host defensive mechanisms against incoming foreign free DNA ends. Therefore, it is important to investigate the involvement of DSB repair pathways in the removal of free DNA ends of linear vector genomes in transduced cells.

In the present study, we investigated the pathways of removal of free ds vector ends by comparing wild-type and SCID mouse hepatocytes transduced with rAAV vectors, or transfected with ds naked linear DNA vectors with an AAV-ITR at each end, by hydrodynamics-based transfection (Nakai *et al.*, 1998, 2001; Liu *et al.*, 1999; Zhang *et al.*, 1999). Although it has not been fully established whether hydrodynamics-based transfection mimics rAAV vector transduction, and AAV-ITR ends of naked ds linear DNA vectors do not necessarily represent free rAAV vector ends which may form T-shaped structures, our present studies demonstrate the presence of three major pathways of free vector end removal: (1) DNA-PKcs–dependent self-circularization, (2) DNA-PKcs–independent self-circularization, and (3) DNA-PKcs–independent concatemerization. Contrary to the previous study in mouse skeletal muscle that showed impaired clearance of free rAAV vector ends in SCID mice (Song *et al.*, 2001), free vector ends were efficiently processed and removed in SCID mouse hepatocytes after rAAV vector injection through the latter two pathways. Our study also suggests the preferential usage of the self-circularization pathways over concatemerization regardless of the presence or the absence of DNA-PKcs activity. Finally, our results show that altering the molecular fate of vector genomes by dysregulation of these pathways affects transgene expression from incoming vectors.

MATERIALS AND METHODS

Construction of rAAV and naked ds linear DNA vectors

The rAAV vector used in this study was based on AAV serotype 2, produced by the triple transfection method (Matsushita *et al.*, 1998), and purified by two cycles of cesium chloride gradient ultracentrifugation followed by ultrafiltration-diafiltration, as previously described (Burton *et al.*, 1999). The physical particle titer was determined by a quantitative dot blot assay (Kessler *et al.*, 1996).

AAV-EF1α-FIX is an rAAV vector that expresses human coagulation factor IX (hF.IX), and was produced based on the plasmid, pAAV-ΔB (Nakai *et al.*, 2000). Briefly, AAV-EF1α-F.IX carried the human elongation factor 1α (EF1α) enhancer-promoter, hF.IX cDNA and the human growth hormone gene polyadenylation signal (polyA).

hF.IX-L+ and L− are ds linear DNA carrying an EF1α-hF.IX expression cassette with (L+) or without (L−) AAV-ITRs as described elsewhere (Nakai *et al.*, 2003a,b). Briefly, plasmid, pVm4.1eδD-hF.IX (Burton *et al.*, 1999) was digested with *Pvu*II to excise the EF1α-hF.IX expression cassette with two AAV-ITRs from the plasmid backbone, then purified by agarose gel fractionation to remove the plasmid backbone sequences. The resulting molecules, hF.IX-L+, consisted of the EF1α-hF.IX expression cassette with a 130-base pair AAV-ITR at each terminal. hF.IX-L− was produced in the same way, starting from a plasmid, pBSδD-hF.IX (Nakai *et al.*, 2003a) that

lacked AAV-ITRs. The EF1α-hF.IX expression cassette carried by hF.IX-L+ and L− was different from that in AAV-EF1α-FIX, in that a 0.62-kb dispensable fragment of the EF1α enhancer-promoter element containing a *Pvu*II site was removed and an additional 0.86-kb fragment of 3′ untranslated region (UTR) of hF.IX cDNA was included. These modifications did not affect transgene expression *in vitro* and *in vivo* (data not shown). All the DNA preparations for *in vivo* use were filtered through a 0.22-μm syringe filter unit.

Animal procedures

Eight-week-old normal female C57BL/6 mice and C57BL/6 CB17 SCID mice were purchased from Jackson Laboratory (Bar Harbor, ME). All animal procedures were performed according to the guidelines for animal care at Stanford University. Portal vein injection of rAAV vector and hydrodynamics-based *in vivo* hepatocyte transfection of naked DNA vectors by tail vein injection were performed as previously described (Nakai *et al*., 1998, 2001; Liu *et al*., 1999; Zhang *et al*., 1999). Blood samples were collected from the retro-orbital plexus.

Measurement of hF.IX in samples

Levels of hF.IX in mouse plasma were measured with an enzyme-linked immunosorbent assay (ELISA) specific for hF.IX using affinity purified plasma hF.IX (Calbiochem, La Jolla, CA) as a standard (Nakai *et al*., 1999).

Southern blot analysis

Total genomic DNA was extracted from livers 6 to 32 weeks after vector injection, and 20 μg of DNA was analyzed for vector copy numbers and molecular forms of vector genomes by Southern blot as previously described (Nakai *et al*., 1999, 2000). The vector genome copy number standards (the number of ds vector genomes [vg] per diploid genomic equivalent [dge]) were 20 μg of naive mouse total liver DNA mixed with the appropriate amount of the corresponding plasmid.

Densitometric analysis

Densitometric analysis of the Southern blots was performed using a G710 Calibrated Imaging Densitometer and Quantity One software (Bio-Rad, Hercules, CA). In order to determine the number of vector genomes per dge, each band intensity was quantified with a non-lane–based method using the Volume Tools. Please note that throughout this paper vector copy number per cell represents an average number of vector genomes in a cell among all the liver cells including vector-genome containing and not containing hepatocytes and nonparenchymal cells. The net vector copy number in vector containing hepatocytes should be much higher than the copy numbers per cell shown in this paper. In rAAV-mediated liver transduction, our estimation, based on a series of our experiments, is that 0.2, 2, and 16 vector copies per cell correspond to approximately 40, 80, and 200 net vector copies per cell, respectively (Nakai *et al*., 2002). The relative amounts of circular monomers and concatemers were determined using the Southern blots of the DNA samples digested with an enzyme that does not cut the vector genomes. Each lane was scanned with 1-mm width and the background noise was subtracted with a lane-based Rolling Disk Background Subtraction method (for details, refer to Quantity One User Guide for Version 4, Bio-Rad), then each band was quantified. The relative amount of circular monomer genomes was estimated by combining the band densities of supercoiled ds circular monomers, ds linear monomers, and relaxed ds circular monomers, while the relative amount of concatemers was estimated by the intensity of the band at a high molecular weight position, and dimers and trimers if present. The rationale of the inclusion of ds linear monomers to estimate the total amount of circular monomer genomes was based on the observation that a portion of circular vector genomes was converted into linear forms because of nonspecific nicking in DNA by digestion with a noncutter enzyme that does not cut the vector genome (Nakai *et al*., 2003a). It should be noted that although approximate estimation of the relative amounts of circular monomers and concatemers was possible, the obtained values may not represent accurate amounts of each form because: (1) in the densitometric analysis we did not take into account that a portion of vector genomes integrate, which may generate a smeared signal on the Southern blots with a noncutter enzyme digestion; (2) electrophoretic mobility of relaxed circular monomers and supercoiled circular dimers is similar (Nakai *et al*., 2003a), which may have overestimated the relative amount of circular monomers in our assay; (3) supercoiled circular DNA may exhibit somewhat impaired hybridization efficiency compared to linear DNA, which might have resulted in underestimation of the relative amount of circular monomers; and (4) a small portion of ds linear monomers on the blots may represent not artificial but true ds linear DNA vector genomes, which have been included in circular monomers in our densitometric analysis.

RESULTS

No difference in transgene expression by rAAV vectors in normal and SCID mice

As a first step toward elucidating the effects of DNA-PKcs on rAAV transduction in the liver, we injected normal and SCID mice with an hF.IX-expressing rAAV vector, AAV-EF1α-F.IX. Eight-week old female C57BL/6 CB17 SCID mice ($n = 5$) and age-matched female normal C57BL/6 mice ($n = 5$) were injected with AAV-EF1α-F.IX at a dose of 2.5×10^{11} vg per mouse via the portal vein. The plasma hF.IX levels were similar between wild-type and SCID mice up to 32 weeks, the length of the study (Fig. 1). This was consistent with previously published results that indicated the SCID mutation does not affect rAAV transduction levels in liver (Snyder *et al*., 1997) and skeletal muscle (Song *et al*., 1998, 2001).

Free rAAV vector ends are efficiently cleared in SCID hepatocytes in vivo *by a mechanism different from that for normal mice*

To determine the molecular fate of rAAV vector genomes in normal and SCID mouse livers, the AAV-EF1α-F.IX–injected mice were sacrificed 32 weeks postinjection, and liver DNA was analyzed by Southern blot. *Bgl*II digestion cleaved vector genomes four times (see vector map in Fig. 2), and was used to determine total vector copy numbers per cell. They were

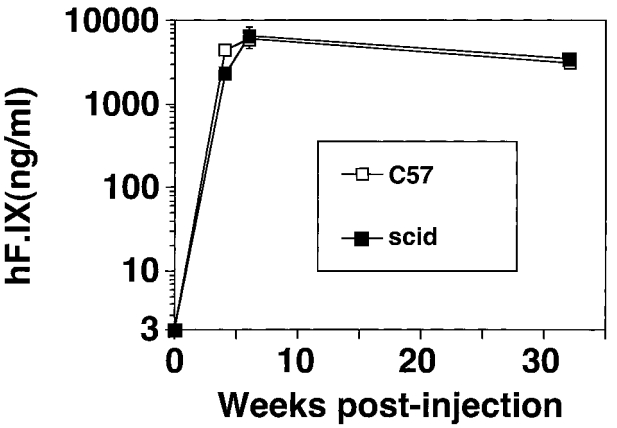

FIG. 1. Transduction efficiency in wild-type and severe combined immunodeficiency (SCID) mice. hF.IX levels in mouse plasma after portal vein injection of AAV-EF1α-F.IX at a dose of 2.5×10^{11} vg per mouse. C57, normal C57BL/6 mice (n = 5); scid, C57BL/6 SCID mice (n = 5). Vertical bars represent mean ± standard errors.

2.45 ± 0.49 and 4.41 ± 0.36 (means ± standard errors) vg/dge in normal and SCID mice, respectively (Fig. 3A, Table 1). The vector copy number per cell was approximately 2-fold higher in SCID mice. (Student's t test, $p = 0.0066$). As shown in Figure 3B, digestion of liver DNA with a single cutter, *Afl*II or *Hin*dIII, revealed head-to-tail, tail-to-tail, and head-to-head concatemers, and no evidence of free vector DNA ends (see Table 2 for the size of each band). Interestingly, in SCID mice, the ratios of "head-to-head to head-to-tail" and "tail-to-tail to head-to-tail" molecules were increased over normal mice. Consistent with this observation, Southern blot analysis with undigested DNA or *Bam*HI-digested DNA (*Bam*HI does not cut the vector genome) and densitometric analysis of the blots clearly demonstrated that there was a larger number of concatemers in SCID mice (Fig. 3C, Table 1). However, estimated circular monomer copy numbers per cell (Table 1) did not show a difference with statistical significance between normal and SCID mice (Student's t test, $p = 0.32$). These results demonstrate that self-circularization was the main pathway of removal of free rAAV vector ends in normal mice, while in SCID mice the concatemerization pathway was more prevalent.

SCID mutation slows and reduces hF.IX expression from naked ds linear DNA vectors transfected into mouse hepatocytes

Next, we investigated the effect of the SCID mutation on transgene expression from naked ds linear DNA vectors delivered to mouse hepatocytes. We injected body weight matched 8-week-old normal C57BL/6 mice (body weight, 18.5 ± 0.6 g, mean ± standard deviation) and C57BL/6 SCID mice (body weight, 18.9 ± 0.7 g) with naked ds linear DNA, hF.IX-L+ (23 μg per mouse, n = 9 each) or hF.IX-L− (22 μg/mouse, n = 10 and 9 for normal and SCID mice, respectively) using a hydrodynamics-based transfection technique. The doses of vectors were determined based on the molecular weights of each vector so that all the mice received an equimolar amount of DNA. hF.IX-L+ represented ds linear rAAV vector genomes while hF.IX-L− served as a control lacking AAV-ITRs. As shown in Figure 4, the kinetics of transgene expression from both hF.IX-L+ and L− was significantly slowed in SCID mice compared to normal mice. Although the difference in plasma hF.IX levels at 6 weeks postinjection in normal and SCID mice injected with hF.IX-L+ was not statistically significant, the levels in the mice injected with hF.IX-L− were significantly lower in SCID mice than in normal mice (Student's t test, p = 0.0017).

A one-time large load of free vector ends are inefficiently processed by self-circularization in SCID mice compared to normal mice

Conversion of incoming ss rAAV genomes into transcriptionally active ds genomes is a slow process that takes approximately 5–6 weeks to go to completion (Miao *et al.*, 1998). Because ds linear DNA vector genomes are highly recombinogenic in hepatocytes, transform into a variety of vector forms within a day (Chen *et al.*, 2001; Nakai *et al.*, unpublished results) and are not always detected in rAAV transduced livers,

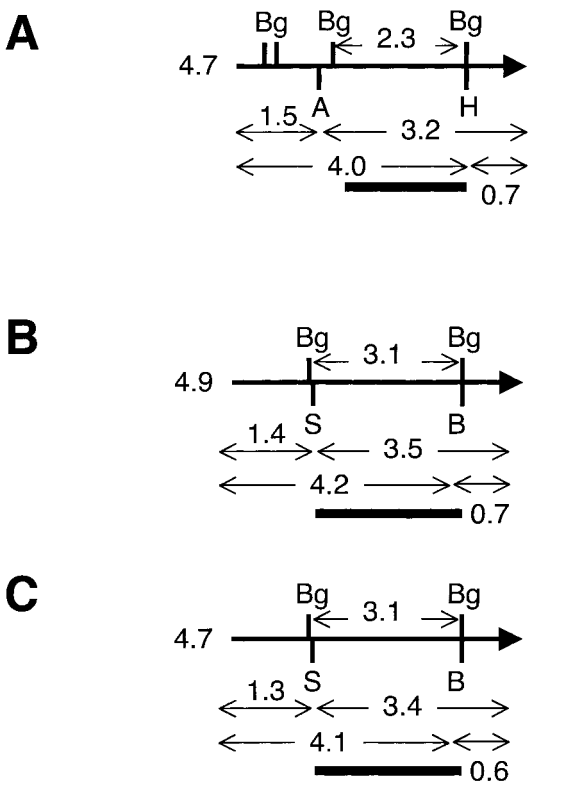

FIG. 2. Restriction enzyme recognition sites in vectors. Diagrams of predicted sizes (kb) of DNA fragments after digestion with restriction enzymes are shown. The main arrows represent one unit of a vector genome. The numbers to the left of the vectors are the full-length of the vector genome (kb). Thick bars indicate probes used in the Southern blot analysis. **A**: AAV-EF1α-F.IX (rAAV vector). **B**: hF.IX-L+ (naked ds DNA). **C**: hF.IX-L− (naked ds DNA). A, *Afl*II; B, *Bam*HI; Bg, *Bgl*II; H, *Hin*dIII; S, *Sac*I.

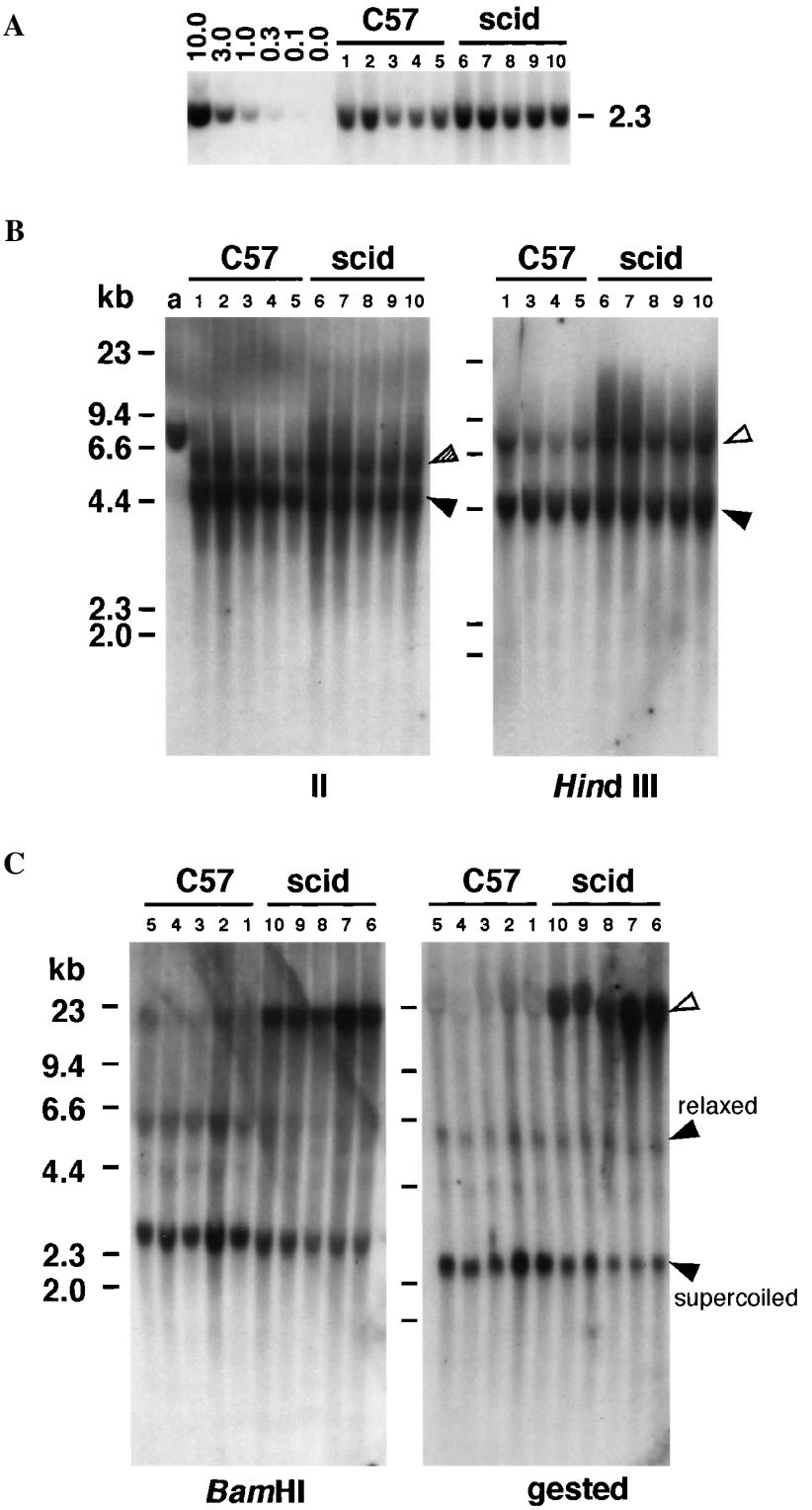

FIG. 3. Southern blot analysis of mouse liver DNA after injection with AAV-EF1α-F.IX. Wild-type C57BL/6 and C57BL/6 severe combined immunodeficiency (SCID) mice were injected via the portal vein with 2.5×10^{11} vg of AAV-EF1α-F.IX, and liver DNA harvested 32 weeks postinjection was analyzed for vector genomes. **A**: *Bgl*II (cuts the vector genome four times) digestion for determination of vector copy number per diploid genomic equivalent (dge); 0.0–10.0 are copy number standards. pAAV-ΔB was used for the standards. **B**: Molecular forms of vector genomes. *Afl*II and *Hin*dIII cut the vector genome only once. Black, open and hatched arrowheads represent head-to-tail, head-to-head and tail-to-tail forms, respectively. Note that no free vector ends were observed (3.2 kb with *Afl*II and 4.0 kb with *Hin*dIII). Lane a is a 1.0 copy number standard (pAAV-ΔB), indicating DNA was digested to completion with the enzyme used, generating a single 7.3-kb band. **C**: Concatemers (indicated with an open arrowhead) and circular monomers (indicated with black arrowheads) present in vector-injected mouse liver. *Bam*HI does not cut the vector genome. C57, normal C57BL/6 mice; scid, C57BL/6 SCID mice. Each lane represents an individual mouse. Identification number of each mouse is shown above the lanes.

Table 1. Relative Amounts of Circular Monomers and Concatemers

Vector	Mouse		Relative amount of each vector form[a] (%)		Total copy number per cell[b] (vg/dge)	Estimated monomer copy number per cell[c] (vg/dge)
			Concatemer	Circular monomer		
AAV-EF1α-F.IX	C57BL/6	1[d]	16	84	3.18	2.67
		2	14	86	3.70	3.18
		3	11	89	1.49	1.33
		4	11	89	1.60	1.42
		5	14	86	2.27	1.95
	Average		**13**	**87**	**2.45**	**2.11**
	SCID	6	64	36	4.92	1.77
		7	76	24	5.28	1.27
		8	66	34	3.44	1.17
		9	61	39	4.37	1.70
		10	41	59	4.06	2.40
	Average		**62**	**38**	**4.41**	**1.66**
hF.IX-L+	C57BL/6	1	77	23	7.00	1.61
		2	82	18	9.55	1.72
	Average		**80**	**21**	**8.28**	**1.67**
	SCID	11	94	6	8.00	0.48
		13	94	6	6.38	0.38
	Average		**94**	**6**	**7.19**	**0.43**
hF.IX-L−	C57BL/6	6	85	15	6.90	1.40
		9	86	14	5.98	0.84
	Average		**86**	**15**	**6.44**	**0.94**
	SCID	17	94	6	6.47	0.39
		20	93	7	8.93	0.63
	Average		**94**	**7**	**7.70**	**0.51**

[a]The relative amount of circular monomers and concatemers in each sample was estimated by densitometry of the Southern blots shown in Figures 3C and 5B. The limitations of this estimation are described in Materials and Methods.

[b]Vector copy number per cell (vector genomes per diploid genomic equivalent [vg/dge]) was determined by densitometry of the blots shown in Figures 3A and 5A.

[c]Estimated circular monomer copy numbers per cell were calculated by multiplying total copy number per cell with the relative amount of circular monomers (%)/100. Please note that although this estimated copy number correlates with the density of each band observed in the blots, it does not necessarily represent the true number of circular genomes as described in Materials and Methods.

[d]These numbers correspond to the mouse identification number in our study.

SCID, severe combined immunodeficiency.

the half life of ds linear rAAV genomes should be short. Considering this slow processing and the relatively short life span, the steady-state concentration of ds linear rAAV vector genomes, at any particular period of time, in hepatocytes is presumed to be small (2.5–4.4 vg/dge over 6 weeks, see above). In contrast, naked ds linear DNA transfection allowed for a considerably large load of free vector ends to be delivered into hepatocytes at one time. The vector copy numbers in C57BL/6 mouse livers 1 day after hF.IX-L+ (23 μg per mouse, $n = 5$) or hF.IX-L− (22 μg/mouse, $n = 4$) injection were 70.12 ± 2.87 vg/dge or 50.94 ± 11.68 vg/dge (means ± standard errors), respectively. Assuming that ds rAAV vector genomes were generated in hepatocytes at a constant rate over a period of 6 weeks, a ds vector load in a rAAV transduced hepatocyte would be approximately 0.1 vg per day, which is 1/700–1/500 of the load in a naked ds linear DNA vector transfected hepatocyte. Therefore, ds linear DNA transfection allowed for investigation of the capacity of processing free DNA vector ends.

Six weeks postinjection, the normal and SCID mice injected with hF.IX-L+ or hF.IX-L− were sacrificed, and liver DNA was analyzed by Southern blot analysis. The number of vector genomes present in the livers of the mice were similar (8.06 ± 0.89 vg/dge in L+/normal; 6.90 ± 0.50 vg/dge in L−/normal; 8.17 ± 0.67 vg/dge in L+/SCID; 7.48 ± 1.20 vg/dge in L−/SCID mice; values are means ± standard errors, $n = 5$ each) (Fig. 5A). As shown in Figure 5B and Table 1, the bands representing circular vector genomes were readily detected in normal mice but barely detected in SCID mice. Southern blot analysis with a single cutter enzyme (*Sac*I or *Bam*HI) revealed that most but not all of the free vector ends were cleared mainly by concatemerization (Fig. 5C). An insignificant amount of free vector ends was observed, but there was no significant difference in the amount of free vector ends in normal and SCID mice. This suggests that the presence of free vector ends in these mice was not related to the impaired DSB repair pathways. Thus, in SCID mice, a one-time large load of free ends of ds rAAV genomes or ds linear DNA vectors could not be processed into circular monomers as efficiently as in normal mice.

TABLE 2. EXPECTED LENGTHS OF DNA FRAGMENTS OF VARIOUS FORMS OF VECTOR GENOMES IN SOUTHERN BLOT ANALYSIS

Vector	*Enzyme used*	*H-H*[a]	*T-T*[a]	*H-T*[a]	*Free ends*
AAV-EF1α-F.IX	*Afl*II		6.4	4.7	3.2
	*Hin*dIII	8.0		4.7	4.0
hF.IX-L+	*Sac*I		7.0	4.9	3.5
	*Bam*HI	8.4		4.9	4.2
hF.IX-L−	*Sac*I		6.8	4.7	3.4
	*Bam*HI	8.2		4.7	4.1

[a]H-H, head-to-head; T-T, tail-to-tail; H-T, head-to-tail. All the fragment sizes are shown as kilobases (kb).

Real DNA fragment lengths might be shorter than expected because of deletions of vector genome termini at vector-vector junctions (Nakai *et al.*, 1999).

DISCUSSION

Possible roles of DNA-PKcs in the removal of free ds rAAV vector ends

Regardless of the presence or absence of DNA-PKcs, free vector ends were efficiently cleared in mouse hepatocytes through different pathways. We have recently demonstrated that a proportion of rAAV concatemers relative to circular monomer genomes was increased as the vector copy number in cells was increased (Nakai *et al.*, 2002). Therefore, the observed difference in the fate of rAAV genomes in normal and SCID mice (Fig. 3) might simply be attributed to the higher number of vector genomes in SCID hepatocytes compared to the wildtype controls. However, considering that the rAAV dose we used and the observed vector copy numbers per cell were still within a range where circular monomers increased as the vector copy numbers per cell increased (Nakai *et al.*, 2002), the lack of an increase in circular monomers in SCID mice compared to the normal mice implies a relative decrease in circular monomers in SCID mice. To support this, the self-circularization pathway was apparently impaired in the absence of DNA-PKcs when large amounts of free vector ends were loaded into the liver at one time by transfection with naked ds linear DNA vectors with or without AAV-ITRs. Although we cannot fully eliminate the possibility that the hydrodynamics-based transfection technique might have affected the processing of incoming vector genomes, our results suggested that there was an alternative self-circularization pathway in the absence of DNA-PKcs. Such an alternative mechanism(s) might be the single-strand annealing or homologous recombination DSB repair pathway because the double-D AAV-ITR structure is frequently observed in self-circularized vector-vector junctions (Duan *et al.*, 1999).

The reason why the amount of circular monomer genomes was not significantly lower in SCID mice than normal mice after rAAV vector administration if DNA-PKcs was involved in rAAV self-circularization, as was observed in naked ds linear DNA vector-injected mice, can be explained. One possible explanation is that in rAAV transduction in SCID mice, a DNA-PKcs–independent alternative self-circularization pathway(s)

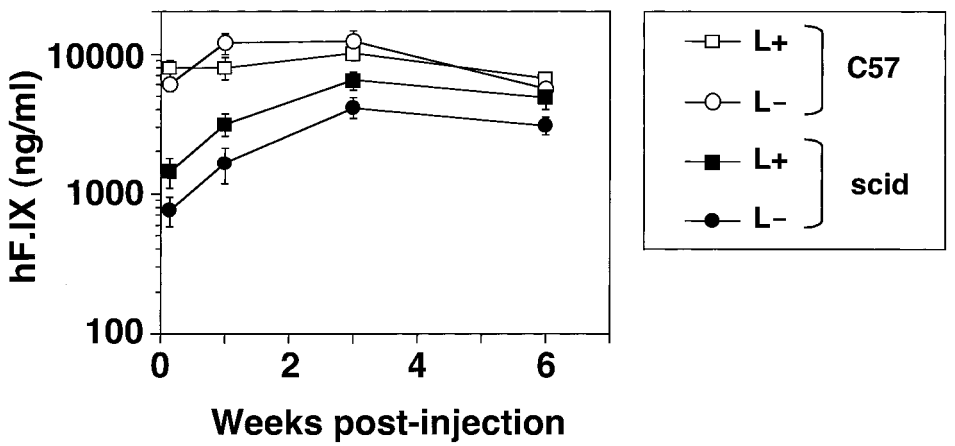

FIG. 4. hF.IX levels in mouse plasma after tail vein injection of naked double-stranded (ds) linear DNA. Normal and severe combined immunodeficiency (SCID) mice were injected with hF.IX-expressing naked ds linear DNA, hF.IX-L+ (23 μg per mouse, $n = 9$ each) or hF.IX-L− (22 μg per mouse, $n = 10$ for normal and $n = 9$ for SCID mice), using a hydrodynamics-based transfection method. Note that elevation of hF.IX levels in SCID mice was significantly slower than in normal mice. C57, normal C57BL/6 mice; scid, C57BL/6 SCID mice. Vertical bars represent mean ± standard errors.

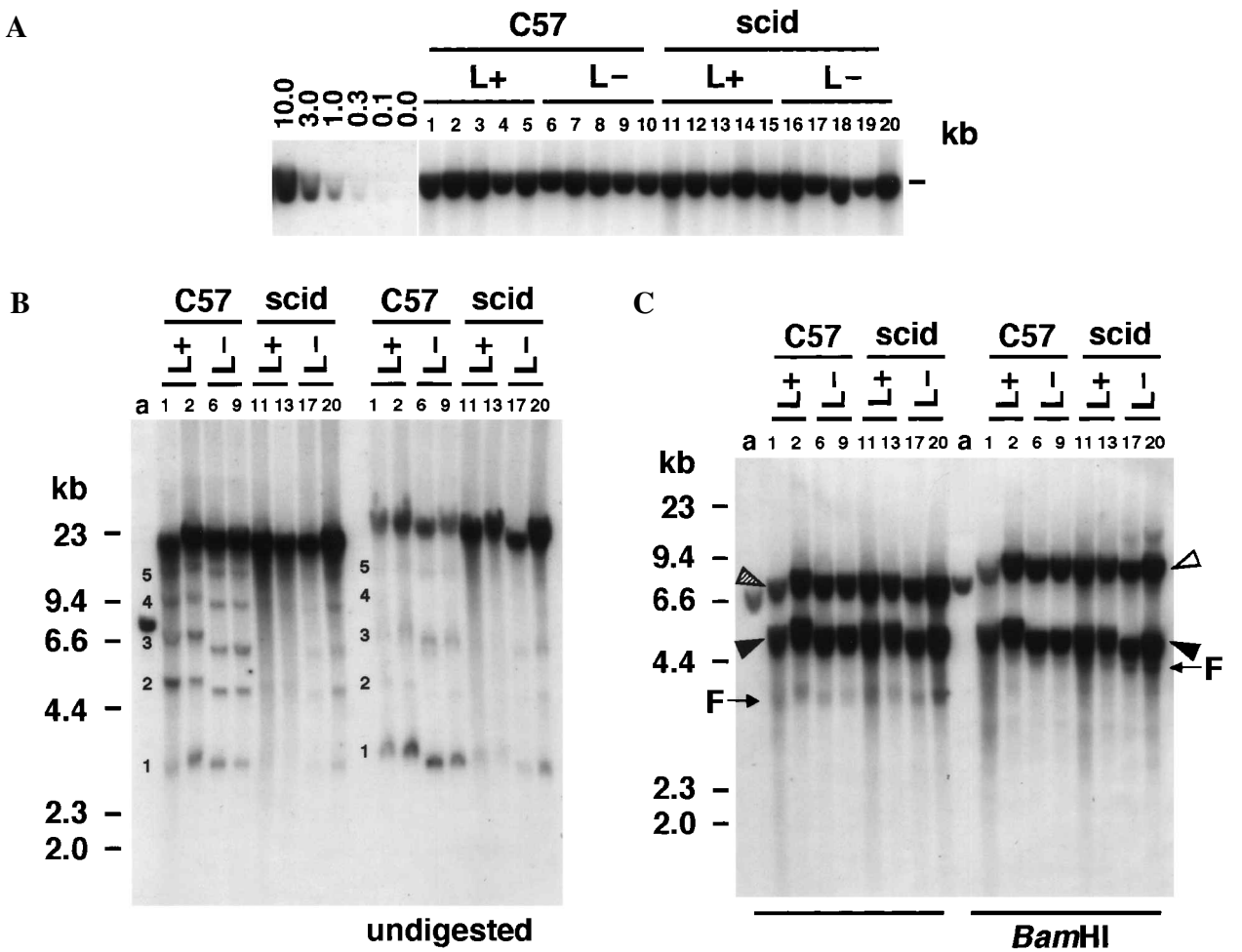

FIG. 5. Southern blot analysis of mouse liver DNA isolated after injection with naked double-stranded (ds) linear DNA. Normal and SCID mouse hepatocytes were transfected with 22–23 μg of naked ds linear DNA as described in the text. Mouse liver DNA harvested 6 weeks postinjection was analyzed for vector genomes by Southern blot. **A**: *Bgl*II (cuts the vector genome twice) digestion for determining vector copy number per diploid genomic equivalent (dge); 0.0–10.0 are copy number standards (pVm4.1eδD-hF.IX). **B**: Concatemers and circular monomers present in ds linear DNA-transfected mouse liver. *Kpn*I does not cut the vector genome. Several discrete bands numbered 1 to 5, are presumed to be as follows based on our observations (Nakai *et al.*, 1999, 2000, 2001, 2003a): 1, supercoiled ds circular monomers; 2, ds linear monomers (likely monomer circles broken at one site during restriction enzyme digestion); 3, relaxed ds circular monomers and/or supercoiled ds circular dimers; 4, ds linear dimers (likely dimer circles broken at one site); and 5, relaxed ds circular dimers and/or supercoiled ds circular trimers. Note that these circles are present at significantly higher levels in normal mice than in SCID mice. **C**: The presence of a small amount of free vector ends in both normal and SCID mice. *Sac*I and *Bam*HI cut the vector genome only once. Arrows with "F" indicate free vector ends. Black, open, and hatched arrowheads represent head-to-tail, head-to-head, and tail-to-tail forms, respectively. Lanes a are 1.0 copy number standards (pBSδD-hF.IX), which indicate DNA was digested to completion with the enzymes used. The sizes of the products from pBSδD-hF.IX digested with *Kpn*I, *Sac*I, and *Bam*HI, which can be detected with this analysis, are 7.6 kb, 6.4 kb, and 7.0 kb, respectively. C57, normal C57BL/6 mice; scid, C57BL/6 SCID mice. Each lane represents an individual mouse. Identification number of each mouse is shown above the lanes.

may continuously remove a small fraction of slowly loaded free rAAV vector ends over time, resulting in the generation of a significant amount of circular monomer genomes by the time transgene expression reaches a plateau (or during 5–6 weeks after vector injection). However, if large amounts of ds linear DNA molecules were delivered at one time, this process would only remove a negligible amount of free vector ends over a limited period of time. Alternatively, AAV-ITR structures in ds rAAV vector genomes may form more preferable substrates for self-circularization than AAV-ITRs in naked ds linear DNA vectors. Because the CB17 SCID mutation generates a potentially partially active mutant enzyme (Blunt *et al.*, 1996; Danska *et al.*, 1996) and has been known to be leaky (Kotloff *et al.*, 1993; Nonoyama *et al.*, 1993), it is also possible that incomplete inactivation of the NHEJ DSB repair pathway might have allowed for self-circularization to some extent in SCID mice.

In contrast to impaired intramolecular self-circularization of linear vector genomes, intermolecular recombination was not

at all affected by the SCID mutation. These results suggest that intramolecular self-circularization and intermolecular concatemerization of rAAV vector genomes are differentially regulated by cellular factors, although these two pathways appear to be similar in that they involve free end joining of DNA vector genomes.

In the naked ds linear DNA vector-injected mice, we observed a small quantity of free vector ends, which might still be detrimental to cells because a single DSB present in extrachromosomal DNA has been reported to be lethal (Bennett *et al.*, 1993). At this time, it is not clear why hepatocytes with unrepaired free vector ends could survive in our study. The quiescent nature of hepatocytes might have allowed for escape from DSB-induced toxicity as suggested by Baekelandt and colleagues (Baekelandt *et al.*, 2000). Alternatively, it is possible that all the concatemers were circular forms and all the free vector ends were derived from input ds linear monomer DNA vector genomes that persist but are not identified as a DSB signal by the cells because of their possible localization in cytoplasm or in a protected niche within nuclei.

Possible effects of DNA-PKcs on rAAV vector transduction in the liver

The present study showed that the SCID mutation altered the molecular fate of rAAV vector genomes and resulted in higher transduction efficiencies as determined by vector copy numbers per cell. However, past as well as the present studies demonstrate that the SCID mutation did not affect rAAV transduction efficiency as determined by transgene expression (Snyder *et al.*, 1997; Song *et al.*, 1998, 2001). On the other hand, when ds linear DNA vectors were transfected into mouse hepatocytes, transgene expression was slowed and reduced in the SCID mice. It is not clear why the SCID mutation affected transgene expression from naked ds linear DNA vectors but not from rAAV vectors. One possible explanation is the difference in the amount of circular monomer genomes between wild-type and SCID mice. This difference was not significant in rAAV vector-injected mice, although it was significant in ds linear DNA vector-injected mice. We have recently demonstrated that an increase in the number of circular monomer rAAV genomes per cell correlates with an increase in transgene expression, while an increase in the number of concatemeric rAAV vector genomes per cell does not necessarily result in a proportional increase in transgene expression in mouse hepatocytes *in vivo* (Nakai *et al.*, 2002). This observation implies that concatemers are not as potent as circular monomers for transgene expression. Thus, although we did not see a substantial difference in transgene expression in rAAV-injected normal and SCID mice, the lack of DNA-PKcs has a potential to affect transgene expression by altering molecular fates of vector genomes.

A model for the pathways of free rAAV vector end removal

The present study demonstrated three distinct pathways of free vector end removal (i.e., DNA-PKcs–independent self-circularization, DNA-PKcs–dependent self-circularization and DNA-PKcs–independent concatemerization). Our study suggested that each pathway has a different capacity. The first pathway, with the smallest capacity, processed a portion of the slowly-loaded free vector ends but could not process large amounts of free ends when they were delivered at high concentration to overload the cells. The second pathway, with an intermediate capacity, processed most of the slowly loaded free vector ends and a proportion of the overloaded ones. The last pathway, with the largest capacity, processed most of the overloaded free vector ends. In addition, considering that concatemers are normally accompanied by circular monomers, and self-circularization could occur by itself without concatemerization (Nakai *et al.*, 2002), the pathways of free DNA end removal are presumed to be hierarchically organized such that self-circularization is preferred over concatemerization.

Based on our observations from past and present studies (Miao *et al.*, 1998; Nakai *et al.*, 1998, 1999, 2000, 2002, 2003a,b), we propose a model for how free rAAV vector ends are removed in hepatocytes *in vivo*. During loading of free rAAV vector ends (i.e., slow transduction process over 5–6 weeks), free vector end clearance first begins to occur by self-circularization. At low vector concentration per cell, self-circularization is favored (Nakai *et al.*, 2002), because concatemerization requires at least two vector genomes per cell (Nakai *et al.*, 2000, 2002). Unlike retroviruses that can remove free ends by self-circularization and integration (Li *et al.*, 2001), the integration efficiency of rAAV is very low (Nakai *et al.*, 2001, 2002), therefore integration does not play a major role. When the concentration of vector genomes is increased, hepatocytes exert the self-circularization pathways until the capacity of those pathways reaches a maximum. If the self-circularization and concatemerization pathways were equally used to remove free vector ends, the ratio of the amount of circular monomers and concatemers should be maintained regardless of the number of input vector genomes with free ends, however this does not occur (Nakai *et al.*, 2002). If concatemerization was the preferred pathway, concatemers should be present in the absence of circular monomers, but this was not the case. Concatemerization occurs only when vector genomes are present in excess (Nakai *et al.*, 2002) or beyond the capacity of self-circularization. In a separate study, we injected another hF.IX-expressing rAAV vector, AAV-CM1 (Nakai *et al.*, 2001) into normal and SCID mice via the portal vein, and performed the same analyses. At lower transduction levels of approximately 1 copy per cell (the net vector copy number in a vector-containing hepatocyte is presumed to be 40–80 copies per cell; see Materials and Methods), most of the vector genomes were circular monomers both in normal and SCID mice (data not shown). Therefore, the preferential use of the circularization pathway appears to occur even when DNA-PKcs is deficient.

The capacity of the DNA-PKcs-independent alternative self-circularization pathway is very limited compared to the DNA-PKcs-dependent pathway. It is robust enough to generate a considerable amount of circular genomes from slowly processed rAAV vector genomes, but is readily saturated with a one-time large load of incoming free ends, generating only a negligible amount of circular molecules in SCID mice.

In conclusion, our present study further supports a recent finding that DNA-PKcs–dependent NHEJ DSB repair pathway is involved in the processing of rAAV genomes in transduced cells, and demonstrates that there is a compensatory genome processing pathway(s) in the absence of DNA-PKcs. Understanding the molecular basis of rAAV transduction, especially

focusing on cellular factors participating in the processing of rAAV vector genomes is essential to further improve rAAV vector strategies. Elucidation of the molecular pathways for genome processing may allow us to regulate vector genome self-circularization, concatemerization, or even integration, making a new generation of rAAV vectors.

ACKNOWLEDGMENT

We thank Leonard Meuse for technical assistance. This work was supported by National Institutes of Health grant RO1-HL64274.

REFERENCES

ALEXANDER, I.E., RUSSELL, D.W., and MILLER, A.D. (1994). DNA-damaging agents greatly increase the transduction of nondividing cells by adeno-associated virus vectors. J. Virol. **68,** 8282–8287.

ALEXANDER, I.E., RUSSELL, D.W., SPENCE, A.M., and MILLER, A.D. (1996). Effects of gamma irradiation on the transduction of dividing and nondividing cells in brain and muscle of rats by adeno-associated virus vectors. Hum. Gene Ther. **7,** 841–850.

ARRUDA, V.R., FIELDS, P.A., MILNER, R., WAINWRIGHT, L., DE MIGUEL, M.P., DONOVAN, P.J., HERZOG, R.W., NICHOLS, T.C., BIEGEL, J.A., RAZAVI, M., DAKE, M., HUFF, D., FLAKE, A.W., COUTO, L., KAY, M.A., and HIGH, K.A. (2001). Lack of germline transmission of vector sequences following systemic administration of recombinant AAV-2 vector in males. Mol. Ther. **4,** 586–592.

BAEKELANDT, V., CLAEYS, A., CHEREPANOV, P., DE CLERCQ, E., DE STROOPER, B., NUTTIN, B., and DEBYSER, Z. (2000). DNA-dependent protein kinase is not required for efficient lentivirus integration. J. Virol. **74,** 11278–11285.

BENNETT, C.B., LEWIS, A.L., BALDWIN, K.K., and RESNICK, M.A. (1993). Lethality induced by a single site-specific double-strand break in a dispensable yeast plasmid. Proc. Natl. Acad. Sci. U.S.A. **90,** 5613–5617.

BLUNT, T., GELL, D., FOX, M., TACCIOLI, G.E., LEHMANN, A.R., JACKSON, S.P., and JEGGO, P.A. (1996). Identification of a nonsense mutation in the carboxyl-terminal region of DNA-dependent protein kinase catalytic subunit in the SCID mouse. Proc. Natl. Acad. Sci. U.S.A. **93,** 10285–10290.

BOSMA, G.C., CUSTER, R.P., and BOSMA, M.J. (1983). A severe combined immunodeficiency mutation in the mouse. Nature **301,** 527–530.

BURTON, M., NAKAI, H., COLOSI, P., CUNNINGHAM, J., MITCHELL, R., and COUTO, L. (1999). Coexpression of factor VIII heavy and light chain adeno-associated viral vectors produces biologically active protein. Proc. Natl. Acad. Sci. U.S.A. **96,** 12725–12730.

CHEN, Z.Y., YANT, S., HE, C.Y., MEUSE, L., SHEN, S., and KAY, M.A. (2001). Linear DNAs concatemerize in vivo and result in sustained transgene expression in mouse liver. Mol. Ther. **3,** 403–410.

COFFIN, J.M., and ROSENBERG, N. (1999). Retroviruses. Closing the joint. Nature **399,** 413–416.

DANIEL, R., KATZ, R.A., and SKALKA, A.M. (1999). A role for DNA-PK in retroviral DNA integration. Science **284,** 644–647.

DANIEL, R., KATZ, R.A., MERKEL, G., HITTLE, J.C., YEN, T.J., and SKALKA, A.M. (2001). Wortmannin potentiates integrase-mediated killing of lymphocytes and reduces the efficiency of stable transduction by retroviruses. Mol. Cell. Biol. **21,** 1164–1172.

DANSKA, J.S., HOLLAND, D.P., MARIATHASAN, S., WILLIAMS, K.M., and GUIDOS, C.J. (1996). Biochemical and genetic defects in the DNA-dependent protein kinase in murine SCID lymphocytes. Mol. Cell. Biol. **16,** 5507–5517.

DUAN, D., SHARMA, P., YANG, J., YUE, Y., DUDUS, L., ZHANG, Y., FISHER, K.J., and ENGELHARDT, J.F. (1998). Circular intermediates of recombinant adeno-associated virus have defined structural characteristics responsible for long-term episomal persistence in muscle tissue. J. Virol. **72,** 8568–8577.

DUAN, D., YAN, Z., YUE, Y., and ENGELHARDT, J.F. (1999). Structural analysis of adeno-associated virus transduction circular intermediates. Virology **261,** 8–14.

HUANG, L.C., CLARKIN, K.C., and WAHL, G.M. (1996). Sensitivity and selectivity of the DNA damage sensor responsible for activating p53-dependent G1 arrest. Proc. Natl. Acad. Sci. U.S.A. **93,** 4827–4832.

KAY, M.A., MANNO, C.S., RAGNI, M.V., LARSON, P.J., COUTO, L.B., MCCLELLAND, A., GLADER, B., CHEW, A.J., TAI, S.J., HERZOG, R.W., ARRUDA, V., JOHNSON, F., SCALLAN, C., SKARSGARD, E., FLAKE, A.W., and HIGH, K.A. (2000). Evidence for gene transfer and expression of factor IX in haemophilia B patients treated with an AAV vector. Nat. Genet. **24,** 257–261.

KESSLER, P.D., PODSAKOFF, G.M., CHEN, X., MCQUISTON, S.A., COLOSI, P.C., MATELIS, L.A., KURTZMAN, G.J., and BYRNE, B.J. (1996). Gene delivery to skeletal muscle results in sustained expression and systemic delivery of a therapeutic protein. Proc. Natl. Acad. Sci. U.S.A. **93,** 14082–14087.

KOTLOFF, D.B., BOSMA, M.J., and RUETSCH, N.R. (1993). V(D)J recombination in peritoneal B cells of leaky SCID mice. J. Exp. Med. **178,** 1981–1994.

LI, L., OLVERA, J.M., YODER, K.E., MITCHELL, R.S., BUTLER, S.L., LIEBER, M., MARTIN, S.L., and BUSHMAN, F.D. (2001). Role of the non-homologous DNA end joining pathway in the early steps of retroviral infection. EMBO J. **20,** 3272–3281.

LIU, F., SONG, Y., and LIU, D. (1999). Hydrodynamics-based transfection in animals by systemic administration of plasmid DNA. Gene Ther. **6,** 1258–1266.

MALIK, A.K., MONAHAN, P.E., ALLEN, D.L., CHEN, B.G., SAMULSKI, R.J., and KURACHI, K. (2000). Kinetics of recombinant adeno-associated virus-mediated gene transfer. J. Virol. **74,** 3555–3565.

MATSUSHITA, T., ELLIGER, S., ELLIGER, C., PODSAKOFF, G., VILLARREAL, L., KURTZMAN, G.J., IWAKI, Y., and COLOSI, P. (1998). Adeno-associated virus vectors can be efficiently produced without helper virus. Gene Ther. **5,** 938–945.

MIAO, C.H., SNYDER, R.O., SCHOWALTER, D.B., PATIJN, G.A., DONAHUE, B., WINTHER, B., and KAY, M.A. (1998). The kinetics of rAAV integration in the liver. Nat. Genet. **19,** 13–15.

NAKAI, H., HERZOG, R.W., HAGSTROM, J.N., WALTER, J., KUNG, S.H., YANG, E.Y., TAI, S.J., IWAKI, Y., KURTZMAN, G.J., FISHER, K.J., COLOSI, P., COUTO, L.B., and HIGH, K.A. (1998). Adeno-associated viral vector-mediated gene transfer of human blood coagulation factor IX into mouse liver. Blood **91,** 4600–4607.

NAKAI, H., IWAKI, Y., KAY, M.A., and COUTO, L.B. (1999). Isolation of recombinant adeno-associated virus vector-cellular DNA junctions from mouse liver. J. Virol. **73,** 5438–5447.

NAKAI, H., STORM, T.A., and KAY, M.A. (2000). Recruitment of single-stranded recombinant adeno-associated virus vector genomes and intermolecular recombination are responsible for stable transduction of liver *in vivo*. J. Virol. **74,** 9451–9463.

NAKAI, H., YANT, S.R., STORM, T.A., FUESS, S., MEUSE, L., and KAY, M.A. (2001). Extrachromosomal recombinant adeno-associated virus vector genomes are primarily responsible for stable liver transduction *in vivo*. J. Virol. **75,** 6969–6976.

NAKAI, H., THOMAS, C.E., STORM, T.A., FUESS, S., POWELL,

S., WRIGHT, J.F., and KAY, M.A. (2002). A limited number of transducible hepatocytes restricts a wide-range linear vector dose response in recombinant adeno-associated virus-mediated liver transduction. J. Virol. **76,** 11343–11349.

NAKAI, H., FUESS, S., STORM, T.A., MEUSE, L., and KAY, M.A. (2003a). Free DNA ends are essential for concatemerization of synthetic double-stranded adeno-associated virus vector genomes transfected into mouse hepatocytes *in vivo*. Mol. Ther. **7,** 112–121.

NAKAI, H., MONTINI, E., FUESS, S., STORM, T.A., MEUSE, L., FINEGOLD, M., GROMPE, M., and KAY, M.A. (2003b). Helper-independent and AAV-ITR-independent chromosomal integration of double-stranded linear DNA vectors in mice. Mol. Ther. **7,** 101–111.

NONOYAMA, S., SMITH, F.O., BERNSTEIN, I.D., and OCHS, H.D. (1993). Strain-dependent leakiness of mice with severe combined immune deficiency. J. Immunol. **150,** 3817–3824.

QING, K., WANG, X.S., KUBE, D.M., PONNAZHAGAN, S., BAJPAI, A., and SRIVASTAVA, A. (1997). Role of tyrosine phosphorylation of a cellular protein in adeno-associated virus 2-mediated transgene expression. Proc. Natl. Acad. Sci. U.S.A. **94,** 10879–10884.

QING, K., HANSEN, J., WEIGEL-KELLEY, K.A., TAN, M., ZHOU, S., and SRIVASTAVA, A. (2001). Adeno-associated virus type 2-mediated gene transfer: role of cellular FKBP52 protein in transgene expression. J. Virol. **75,** 8968–8976.

RAJ, K., OGSTON, P., and BEARD, P. (2001). Virus-mediated killing of cells that lack p53 activity. Nature **412,** 914–917.

SANLIOGLU, S., DUAN, D., and ENGELHARDT, J.F. (1999). Two independent molecular pathways for recombinant adeno-associated virus genome conversion occur after UV-C and E4orf6 augmentation of transduction. Hum. Gene Ther. **10,** 591–602.

SANLIOGLU, S., BENSON, P., and ENGELHARDT, J.F. (2000). Loss of ATM function enhances recombinant adeno-associated virus transduction and integration through pathways similar to UV irradiation. Virology **268,** 68–78.

SMITH, G.C., and JACKSON, S.P. (1999). The DNA-dependent protein kinase. Genes Dev. **13,** 916–934.

SNYDER, R.O., MIAO, C.H., PATIJN, G.A., SPRATT, S.K., DANOS, O., NAGY, D., GOWN, A.M., WINTHER, B., MEUSE, L., COHEN, L.K., THOMPSON, A.R., and KAY, M.A. (1997). Persistent and therapeutic concentrations of human factor IX in mice after hepatic gene transfer of recombinant AAV vectors. Nat. Genet. **16,** 270–276.

SONG, S., MORGAN, M., ELLIS, T., POIRIER, A., CHESNUT, K., WANG, J., BRANTLY, M., MUZYCZKA, N., BYRNE, B.J., ATKINSON, M., and FLOTTE, T.R. (1998). Sustained secretion of human alpha-1-antitrypsin from murine muscle transduced with adeno-associated virus vectors. Proc. Natl. Acad. Sci. U.S.A. **95,** 14384–14388.

SONG, S., LAIPIS, P.J., BERNS, K.I., and FLOTTE, T.R. (2001). Effect of DNA-dependent protein kinase on the molecular fate of the rAAV2 genome in skeletal muscle. Proc. Natl. Acad. Sci. U.S.A. **98,** 4084–4088.

STEDMAN, H., WILSON, J.M., FINKE, R., KLECKNER, A.L., and MENDELL, J. (2000). Phase I clinical trial utilizing gene therapy for limb girdle muscular dystrophy: α-, β-, γ-, or Δ-sarcoglycan gene delivered with intramuscular instillations of adeno-associated vectors. Hum. Gene Ther. **11,** 777–790.

VINCENT-LACAZE, N., SNYDER, R.O., GLUZMAN, R., BOHL, D., LAGARDE, C., and DANOS, O. (1999). Structure of adeno-associated virus vector DNA following transduction of the skeletal muscle. J. Virol. **73,** 1949–1955.

WAGNER, J.A., NEPOMUCENO, I.B., MESSNER, A.H., MORAN, M.L., BATSON, E.P., DIMICELI, S., BROWN, B.W., DESCH, J.K., NORBASH, A.M., CONRAD, C.K., GUGGINO, W.B., FLOTTE, T.R., WINE, J.J., CARTER, B.J., REYNOLDS, T.C., MOSS, R.B., and GARDNER, P. (2002). A phase II, double-blind, randomized, placebo-controlled clinical trial of tgAAVCF using maxillary sinus delivery in patients with cystic fibrosis with antrostomies. Hum. Gene Ther. **13,** 1349–1359.

XIAO, X., LI, J., and SAMULSKI, R.J. (1996). Efficient long-term gene transfer into muscle tissue of immunocompetent mice by adeno-associated virus vector. J. Virol. **70,** 8098–8108.

YANG, J., ZHOU, W., ZHANG, Y., ZIDON, T., RITCHIE, T., and ENGELHARDT, J.F. (1999). Concatamerization of adeno-associated virus circular genomes occurs through intermolecular recombination. J. Virol. **73,** 9468–9477.

ZENTILIN, L., MARCELLO, A., and GIACCA, M. (2001). Involvement of cellular double-stranded DNA break binding proteins in processing of the recombinant adeno-associated virus genome. J. Virol. **75,** 12279–12287.

ZHANG, G., BUDKER, V., and WOLFF, J.A. (1999). High levels of foreign gene expression in hepatocytes after tail vein injections of naked plasmid DNA. Hum. Gene Ther. **10,** 1735–1737.

Address reprint requests to:
Mark A. Kay, M.D., Ph.D.
Departments of Pediatrics and Genetics
Stanford University
300 Pasteur Drive
Room G305A
Stanford, CA 94305

E-mail: markay@stanford.edu

Received for publication January 3, 2002; accepted after revision April 21, 2003.

Published online: May 12, 2003.